OGLE-2003-BLG-238: MICROLENSING MASS ESTIMATE OF AN ISOLATED STAR[1]

Guangfei Jiang,[2] D. L. DePoy,[2] A. Gal-Yam,[3,4] B. S. Gaudi,[5] A. Gould,[2] C. Han,[6]
Y. Lipkin,[7] D. Maoz,[7] E. O. Ofek,[7] B.-G. Park,[8] and R. W. Pogge[2]
(The μFUN Collaboration)

A. Udalski,[9] M. Kubiak,[9] M. K. Szymański,[9] O. Szewczyk,[9] K. Żebruń,[9]
Ł. Wyrzykowski,[7,9] I. Soszyński,[9] and G. Pietrzyński[9,10]
(The OGLE Collaboration)

and

M. D. Albrow,[11] J.-P. Beaulieu,[12] J. A. R. Caldwell,[13,14] A. Cassan,[12] C. Coutures,[12,15] M. Dominik,[16]
J. Donatowicz,[17] P. Fouqué,[18] J. Greenhill,[19] K. Hill,[19] K. Horne,[16] S. F. Jørgensen,[20]
U. G. Jørgensen,[20] S. Kane,[16] D. Kubas,[21] R. Martin,[22] J. Menzies,[23] K. R. Pollard,[11]
K. C. Sahu,[13] J. Wambsganss,[20] R. Watson,[19] and A. Williams[22]
(The PLANET Collaboration[24])

ABSTRACT

Microlensing is the only known direct method to measure the masses of stars that lack visible companions. In terms of microlensing observables, the mass is given by $M = (c^2/4G)\tilde{r}_E\theta_E$ and so requires the measurement of both the angular Einstein radius θ_E and the projected Einstein radius $\tilde{r}_E$. Simultaneous measurement of these two parameters is extremely rare. Here we analyze OGLE-2003-BLG-238, a spectacularly bright ($I_{min} = 10.3$), high-magnification ($A_{max} = 170$) microlensing event. Pronounced finite-source effects permit a measurement of $\theta_E = 650$ μas. Although the timescale of the event is only $t_E = 38$ days, one can still obtain weak constraints on the microlens parallax: 4.4 AU $< \tilde{r}_E < 18$ AU at the 1 σ level. Together these two parameter measurements yield a range for the lens mass of 0.36 $M_\odot < M < 1.48$ $M_\odot$. As was the case for MACHO-LMC-5, the only other single star (apart from the Sun) whose mass has been determined from its gravitational effects, this estimate is rather crude. It does, however, demonstrate the viability of the technique. We also discuss future prospects for single-lens mass measurements.

Subject headings: gravitational lensing — stars: fundamental parameters

[1] Based in part on observations obtained with the 1.3 m Warsaw Telescope at the Las Campanas Observatory of the Carnegie Institution of Washington and the Danish 1.54 m telescope at ESO, La Silla, Chile, operated by Instrumentcenter for Jordbaseret Astronomisk Forskning (IJAF) and financed by Statens Natur-videnskabelige Forskningsråd (SNF).

[2] Department of Astronomy, The Ohio State University, 140 West 18th Avenue, Columbus, OH 43210; jiang@astronomy.ohio-state.edu, depoy@astronomy.ohio-state.edu, gould@astronomy.ohio-state.edu, pogge@astronomy.ohio-state.edu.

[3] Department of Astronomy, California Institute of Technology, Pasadena, CA 91025; avishay@astro.caltech.edu.

[4] Hubble Fellow.

[5] Harvard-Smithsonian Center for Astrophysics, Cambridge, MA 02138; sgaudi@cfa.harvard.edu.

[6] Department of Physics, Institute for Basic Science Research, Chungbuk National University, Chongju 361-763, Korea; cheongho@astroph.chungbuk.ac.kr.

[7] School of Physics and Astronomy and Wise Observatory, Tel Aviv University, Tel Aviv 69978, Israel; yiftah@wise.tau.ac.il, dani@wise. tau.ac.il, eran@wise.tau.ac.il.

[8] Korea Astronomy Observatory 61-1, Whaam-Dong, Youseong-Gu, Daejeon 305-348, Korea; bgpark@boao.re.kr.

[9] Warsaw University Observatory, Al. Ujazdowskie 4, 00-478 Warszawa, Poland; udalski@astrouw.edu.pl, soszynsk@astrouw.edu.pl, wyrzykow@astrouw.edu.pl, mk@astrouw.edu.pl, msz@astrouw.edu.pl, pietrzyn@astrouw.edu.pl, szewczyk@astrouw.edu.pl, zebrun@astrouw.edu.pl.

[10] Departmento de Física, Universidad de Concepcion, Casilla 160-C, Concepcion, Chile; pietrzyn@hubble.cfm.udec.cl.

[11] Department of Physics and Astronomy, University of Canterbury, Private Bag 4800, Christchurch, New Zealand.

[12] Institut d'Astrophysique de Paris, 98bis Boulevard Arago, 75014 Paris, France.

[13] Space Telescope Science Institute, 3700 San Martin Drive, Baltimore, MD 21218.

[14] McDonald Observatory, University of Texas, Box 1337-MCD, Fort Davis, TX 79734.

[15] DSM/DAPNIA, CEA Saclay, 91191 Gif-sur-Yvette Cedex, France.

[16] School of Physics and Astronomy, University of St. Andrews, North Haugh, St. Andrews KY16 9SS, UK.

[17] Department of Computing, Technical University of Vienna, Wiedner Hauptstrasse 10, Vienna, Austria.

[18] Observatoire Midi-Pyrenees, UMR 5572, 14, Avenue Edouard Belin, F-31400 Toulouse, France.

[19] School of Mathematics and Physics, University of Tasmania, Private Bag, Hobart, Tasmania 7001, Australia.

[20] Astronomical Observatory, Niels Bohr Institute, Juliane Maries Vej 30, DK-2100 Copenhagen, Denmark; sfj@astro.ku.dk.

[21] Astrophysik, Universität Potsdam, Am Neuen Palais 10, D-14469 Potsdam, Germany.

[22] Perth Observatory, Walnut Road, Bickley, Perth 6076, Australia.

[23] South African Astronomical Observatory, P.O. Box 9, Observatory, 7935, South Africa.

[24] The PLANET Collaboration can be contacted collectively at planetmembers@anu.edu.au.

1. INTRODUCTION

When microlensing experiments were first proposed (Paczyński 1986) and implemented (Alcock et al. 1993; Aubourg et al. 1993; Udalski et al. 1993), it was not expected to be possible to measure the masses and distances of individual microlenses. The only microlensing parameter that depends on the mass and that is routinely measured is the Einstein timescale t_E, which is a degenerate combination of the lens mass M and the lens-source relative parallax π_{rel} and proper motion μ_{rel}. Specifically,

$$t_E = \frac{\theta_E}{\mu_{rel}}, \quad \theta_E = \sqrt{\kappa M \pi_{rel}}, \quad \kappa \equiv \frac{4G}{c^2 \, AU} \simeq 8.14 \frac{mas}{M_\odot}, \quad (1)$$

where θ_E is the angular Einstein radius. However, Gould (1992) showed that if both θ_E and the microlens parallax,

$$\pi_E = \sqrt{\frac{\pi_{rel}}{\kappa M}}, \quad (2)$$

could be measured, then the mass and lens-source relative parallax could both be determined:

$$M = \frac{\theta_E}{\kappa \pi_E}, \quad \pi_{rel} = \pi_E \theta_E. \quad (3)$$

Nevertheless, of the roughly 2000 microlensing events detected to date, there have been only about a dozen for which θ_E has been measured and a dozen for which π_E has been measured. Moreover, there is only one event, EROS-BLG-2000-5, with measurements of *both* parameters and so for which the microlens mass and distance have been reliably determined (An et al. 2002). Since this one event was a binary, and since all the other stars with directly measured masses are components of binaries, it remains the case today that the only single star with a directly measured mass is the Sun.

The one exception is the microlens in MACHO-LMC-5. Alcock et al. (2001) were able to measure both θ_E and π_E for this event and thus measure the mass and distance. These estimates were completely inconsistent with photometry-based estimates of these quantities, but Gould (2004) resolved this puzzle by showing that the π_E measurement was subject to a discrete degeneracy for this event and that the alternate solution was consistent at the few σ level with the photometric evidence. Drake et al. (2004) then obtained a new trigonometric parallax measurement of this event. Combining this with earlier data, Gould et al. (2004) were able to improve the precision of the mass measurement to 17%.

Here we analyze OGLE-2003-BLG-238, the brightest microlensing event ever observed and only the fourth reported point-lens (i.e., nonbinary) event with pronounced finite-source effects. As with the other three such events (Alcock et al. 1997; Smith et al. 2003b; Yoo et al. 2004), these finite-source effects allow one to measure θ_E with reasonably good ($\sim$10%) precision, where the error is typically dominated by the modeling of the source rather than the microlensing event. Hence, if π_E could also be measured, it would be possible to determine M.

Despite the event's short duration, it is still possible to detect parallax effects in OGLE-2003-BLG-238 because of its bright source and high magnification. For short events like this one, the Earth's acceleration can be approximated as uniform during the event. Gould et al. (1994) showed that under these conditions, the parallax effect reduces to a simple asymmetry in the light curve around the peak. The high magnification of OGLE-2003-BLG-238 permits a very accurate measurement of the peak time of the event, which in turn makes the fitting process very sensitive to this small asymmetry. The brightness of the source allows high-precision photometric measurements even in the wings of the event, which enable detection of these subtle deviations. Unfortunately, as also shown by Gould et al. (1994), the simplicity of the parallax effect for short events implies that only one-dimensional parallax information can be effectively extracted, whereas the microlens parallax is intrinsically a two-dimensional vector π_E. That is, while one component of the vector parallax is well determined, the scalar parallax π_E is not well determined, and this degrades the mass determination through equation (3). Nevertheless, this is still only the second single star (other than the Sun) for which any direct mass measurement at all can be made.

2. OBSERVATIONAL DATA

The microlensing event OGLE-2003-BLG-238 was identified by the OGLE III Early Warning System (EWS; Udalski 2003) on 2003 June 22. It peaked on HJD$' \equiv$ HJD $-$ 2,450,000 $=$ 2878.38 (2003 August 26.88) over South Africa. OGLE III observations were carried out in the I band using the 1.3 m Warsaw Telescope at the Las Campanas Observatory, Chile, which is operated by the Carnegie Institution of Washington. While OGLE III normally operates in survey mode, cycling through the observed fields typically once per two nights during the main part of the "bulge season," it can switch rapidly to follow-up mode if an event is of particular interest and requires dense sampling. The high magnification of OGLE-2003-BLG-238, which was predicted while the event was developing, and possible deviations from a single point mass microlensing light-curve profile were the main reasons that OGLE observed this event in follow-up mode.

The OGLE III data comprise a total of 205 observations in the I band, including 144 during the 2003 season and 61 in the two previous seasons, 2001 and 2002. The exposures were generally the standard 120 s, except for three nights (HJD$'$ 2877.5–2879.7) around the maximum when the star was too bright for the standard exposure time. The time of exposure was adjusted then to the current brightness of the lens and seeing conditions to avoid saturation of images and was as short as 10 s on the night of maximum. Photometry was obtained with the OGLE III image subtraction technique data pipeline (Udalski 2003) based in part on the Woźniak (2000) difference image analysis (DIA) implementation.

OGLE DIA photometry is then transformed to standard magnitudes using the constant flux component of the source star determined from the reference image with the DoPhot photometry program (Schechter et al. 1993) and converted to the DIA flux scale. This aligns the OGLE photometry with DoPhot-based photometry but with generally much higher precision measurements.

Following the alert, the event was monitored by the Microlensing Follow-Up Network (μFUN; Yoo et al. 2004) from sites in Chile and Israel and by the Probing Lensing Anomalies Network (PLANET; Albrow et al. 1998) from sites in Chile and Tasmania. The μFUN Chile observations were carried out at the 1.3 m (ex-2MASS) telescope at Cerro Tololo Inter-American Observatory using the ANDICAM camera, which simultaneously images at optical and infrared wavelengths (DePoy et al. 2003). There were a total 203 images in the I band from HJD$'$ 2870.5 (8 days before peak) until HJD$'$ 2950.5 at the end of the season. The exposures were

generally 300 s but were shortened to 120 s for 81 exposures over the peak. The exposures should have been further shortened on the night of the peak, but due to human error, this did not happen. Hence, all 19 of these images were saturated. μFUN obtained 12 points in V, primarily to determine the source color. This includes one saturated point over the peak. All saturated images were discarded.

The μFUN Israel observations were carried out in the I band using the Wise 1 m telescope at Mitzpe Ramon, 200 km south of Tel Aviv. There were 14 observations in total, all restricted to the peak of the event, $2877.3 < \mathrm{HJD}' < 2883.3$. The exposures (all 240 s) were obtained using the Wise Tektronix 1K CCD camera.

The PLANET Chile observations were carried out in the R band using the Danish 1.54 m telescope at the European Southern Observatory in La Silla, Chile. There were a total of 68 observations from HJD' 2874.6 to HJD' 2883.7. The exposure times ranged from 2 to 80 s. The PLANET Tasmania observations were carried out in the I band using the Canopus 1 m telescope near Hobart, Tasmania, with 52 observations from HJD' 2877.9 to HJD' 2903.9. The exposure times ranged from 60 to 300 s. During the first night in Tasmania the data were taken despite significant cloud cover by observing through "holes" in the cloudy sky. This proved feasible only because of the extreme brightness ($I \sim 11$) of the source and demonstrates the importance of carefully monitoring events in real time to determine whether they should be observed despite truly awful conditions. All μFUN and PLANET photometry were extracted using the PLANET pipeline, which is based on DoPhot.

The position of the source is R.A. $= 17^{\mathrm{h}}45^{\mathrm{m}}50\overset{\mathrm{s}}{.}34$, decl. $= -22°40'58\overset{''}{.}1$ (J2000) ($l, b = 5°.72, 2°.60$), so it was accessible for most of the night near peak from Chile and Tasmania but for only a few hours from Israel. The combined data sets are shown in Figure 1.

3. FINITE-SOURCE EFFECTS

In general, the fluxes, $F_i(t)$, observed during a microlensing event by $i = 1, \ldots, n$ observatory-filter combinations are fit to the form,

$$F_i(t) = F_{s,i}A(t) + F_{b,i}, \qquad (4)$$

where $F_{s,i}$ is the flux of the unmagnified source star as seen by the ith observatory and $F_{b,i}$ is any background flux that lies in the aperture but is not participating in the microlensing event. (The one exception would be a binary-source event, in which case two source-star terms and two magnification functions would be required.)

In most cases, the lensed star can be fairly approximated as a point source. The magnification is then given by (Paczyński 1986)

$$A(u) = \frac{u^2 + 2}{u(u^2 + 4)^{1/2}}, \qquad (5)$$

where u is the angular source-lens separation in units of the angular Einstein radius θ_{E}. However, this approximation breaks down for $u \lesssim \rho$, where

$$\rho \equiv \frac{\theta_*}{\theta_{\mathrm{E}}} \qquad (6)$$

is the angular source size θ_* normalized to θ_{E}. Finite-source effects then dominate. An appropriate formalism for incorpo-

rating these effects is given by Yoo et al. (2004). Here we summarize the essentials. If limb darkening is neglected, the total magnification becomes (Gould 1994; Witt & Mao 1994; Yoo et al. 2004)

$$A_{\mathrm{uni}}(u|\rho) \simeq A(u)B_0(u/\rho), \quad B_0(z) \equiv \frac{4}{\pi}zE(k,z), \qquad (7)$$

where E is the elliptic integral of the second kind and $k = \min(z^{-1}, 1)$. This formula is accurate to $O(\rho^2/8)$ (Yoo et al. 2004), and hence it applies whenever (as in the present case) $\rho \ll 1$. Note from Figure 1 that the finite-source fit passes first above the point-source curve and then moves below it. This transition occurs when $B_0(z) = 1$, which (from Fig. 3 of Yoo et al. 2004) occurs at $z \sim 0.54$. In contrast, for MACHO-95-30 (Alcock et al. 1997) and OGLE-2003-BLG-262 (Yoo et al. 2004) the finite-source fits remain above the point-source curves throughout, because in those cases the minimum source-lens separation (impact parameters) were $u_0 \sim 0.7\rho$ and $u_0 \sim 0.6\rho$, respectively.

To include the effects of limb darkening, we model the source profile S_λ at each wavelength λ by

$$S_\lambda(\vartheta) = \overline{S}_\lambda \left[1 - \Gamma_\lambda \left(1 - \frac{3}{2} \cos \vartheta \right) \right], \qquad (8)$$

where Γ_λ is the linear limb-darkening coefficient and ϑ is the angle between the normal to the stellar surface and the line of sight. The magnification is then given by

$$A_{\mathrm{ld}}(u|\rho) = A(u)[B_0(z) - \Gamma B_1(z)], \qquad (9)$$

where $B_1(z)$ is a function described by equation (16) and Figure 3 of Yoo et al. (2004).

4. PARALLAX EFFECT

If the motions of the source, lens, and observer can all be approximated as rectilinear, the source-lens separation u in equation (5) can be written as

$$u(t) = \sqrt{[\tau(t)]^2 + [\beta(t)]^2}, \qquad (10)$$

where

$$\tau(t) = \frac{t - t_0}{t_{\mathrm{E}}}, \qquad \beta(t) = u_0. \qquad (11)$$

The simplest point-source fit to a microlensing event requires five parameters: the source flux F_s, the background flux F_b, the time of closest approach t_0, the Einstein timescale t_{E}, and impact parameter u_0.

However, even if the source and lens can be assumed to be in rectilinear motion, the Earth is not. Especially for the long events [$t_{\mathrm{E}} \geq (1/2\pi)$ yr], the Earth parallax effect must be taken into account. The event OGLE-2003-BLG-238 lasted only 38 days, and hence parallax effects would be negligible if the source were not very bright and highly magnified, both of which facilitate detection of the very subtle parallax effect. Moreover, after it was realized that finite-source effects had been detected, both OGLE and μFUN intensified observations of the event in the hope of measuring the parallax and so combining the result with the source-size measurement to determine a mass.
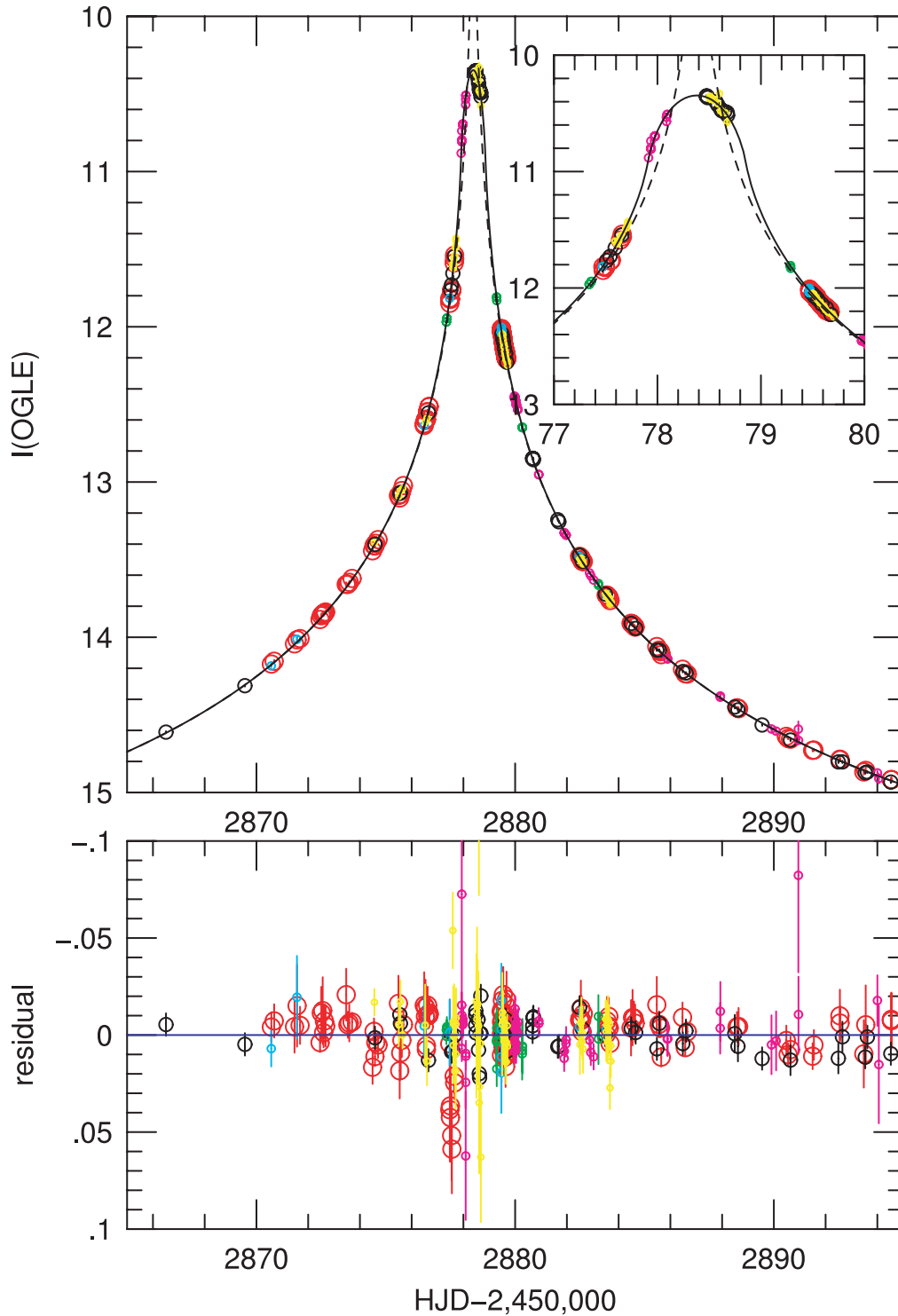
FIG. 1.—Photometry of microlensing event OGLE-2003-BLG-238 near its peak on 2003 August 26.88 (HJD 2,452,878.38). Data points are in I (OGLE: *black*; μFUN Chile: *red*; PLANET Tasmania: *magenta*; μFUN Israel: *green*), V (μFUN: *cyan*), and R (PLANET Chile: *yellow*). The saturated and other excluded points are not shown. The circles are displayed at different sizes to make the figure more readable. All bands are linearly rescaled so that F_s and F_b are the same as the OGLE observations, which define the magnitude scale. The solid curve shows the best-fit nonparallax model with finite-source effect. The dashed curve shows the light curve expected for the same lens model but with a point source.

Historically, parallax fits were carried out in the heliocentric frame. That is, u_0 was adopted as the point of closest approach to the Sun, and t_0 was the time at which this approach occurred. When, as in the present case, parallax is only weakly detected, the trajectory relative to the Sun is poorly determined, so t_0 and u_0 have very large errors that are highly correlated with the

parallax parameters. In the geocentric frame, in contrast, t_0 and u_0 are directly determined from the time and height of the peak of the light curve (Dominik 1998). Gould (2004) further refined the geocentric frame by subtracting out the Earth-Sun relative velocity as well as their positional offset. This frame is appropriate for the analysis of OGLE-2003-BLG-238. Hence, we

TABLE 1
OGLE-2003-BLG-238 Fit Parameters

Parameters	Parallax Fit		Nonparallax Fit	
	Value	Error	Value	Error
t_0 (days)............................	2878.38123	0.00078	2878.38026	0.00076
u_0......................................	0.00200	0.00021	0.00222	0.00019
t_E (days)	38.18743	0.22142	37.58892	0.18946
ρ	0.01282	0.00012	0.01299	0.00012
Γ_I..	0.47696	0.06007	0.46658	0.05793
Γ_R	0.53287	0.08419	0.52438	0.08308
$\pi_{E,N}$	-0.02053	0.19697	0.0	...
$\pi_{E,E}$....................................	0.06639	0.01328	0.0	...
$\pi_{E,\parallel}$	0.06700	0.01181	0.0	...
$\pi_{E,\perp}$	0.01847	0.19706	0.0	...
$(F_b/F_s)_{I_1}$	-0.03716	0.00763	-0.05265	0.00549
$(F_b/F_s)_{I_2}$	0.00959	0.00704	-0.01235	0.00479
$(F_b/F_s)_{V_2}$	-0.00594	0.10906	-0.02527	0.07587
$(F_b/F_s)_{I_3}$	0.02762	0.08100	0.02850	0.05617
$(F_b/F_s)_{I_4}$	-0.07444	0.02112	-0.09285	0.01485
$(F_b/F_s)_{R_4}$	-0.14948	0.04248	-0.16968	0.02990
χ^2..	478.323	...	510.643	...

Note.—Observatories: 1=OGLE, 2=μFUN Chile, 3=μFUN Israel, 4=PLANET; $\Delta\chi^2 \simeq 32$.

follow the Gould (2004) formalism for modeling parallax in the geocentric frame.

The parallax effect is parameterized by a vector π_E whose magnitude gives the ratio of the Earth's orbit (1 AU) to the size of the Einstein ring projected onto the observer plane ($\tilde{r}_E$) and whose direction is that of the lens-source relative motion as seen from the Earth at the peak of the event. Explicitly, $\pi_E \equiv$ AU/$\tilde{r}_E$. Equation (11) is then replaced by

$$\tau(t) = \frac{t - t_0}{t_E} + \delta\tau, \quad \beta(t) = u_0 + \delta\beta, \quad (12)$$

where

$$(\delta\tau, \delta\beta) = \pi_E \Delta s = (\pi_E \cdot \Delta s, \pi_E \times \Delta s) \quad (13)$$

and Δs is the apparent position of the Sun relative to what it would be if the Earth remained in rectilinear motion with the velocity it had at the peak of the event (see eqs. [4]–[6] of Gould 2004). More explicitly,

$$(\delta\tau, \delta\beta) = [\Delta s_N(t)\pi_{E,N} + \Delta s_E(t)\pi_{E,E}, \\ - \Delta s_N(t)\pi_{E,E} + \Delta s_E(t)\pi_{E,N}], \quad (14)$$

where the subscripts N and E refer to components projected on the sky in north and east celestial coordinates.

A major advantage of this formalism is that the parameters t_0, u_0, and t_E are virtually the same for the parallax and nonparallax solutions and, especially important in the present case, when the parallax solution is varied in the π_E plane to obtain likelihood contours.

4.1. Nonparallax Fit

As we will show in § 4.2, the parallax effect is quite subtle and so can, to a first approximation, be ignored. On the other hand, the finite-source effects are quite severe (see Fig. 1). We therefore begin by fitting the light curve by taking into account finite-source effects (including linear limb darkening) but not parallax. The fit therefore contains six geometric parameters

$(t_0, u_0, t_E, \rho, \Gamma_I, \Gamma_R)$ as well as 12 flux parameters (two for each observatory-filter combination). The results are listed in Table 1 and plotted in Figure 1. Also shown in Figure 1 is the light curve that would have been generated by the same event but assuming that the source had been a point of light. As discussed in § 3, this remains below the finite-source curve until $z \equiv u/\rho = 0.54$ and then rises dramatically above it.

4.2. Parallax Fit

To find the best-fit parallax π_E and the error ellipse around it, we conduct a grid search over the π_E plane. That is, we minimize χ^2 by holding each trial parameter pair $\pi_E \equiv (\pi_{E,N}, \pi_{E,E})$ fixed while allowing the remaining 18 parameters (see § 4.1) to vary. After finding the best-fit π_E, we hold this fixed and renormalize the errors so that χ^2 per degree of freedom is unity. We eliminate the largest outlier point and repeat the process until there are no 3 σ outliers. Of course, we first eliminate the 19 saturated points in μFUN Chile I and one saturated point in μFUN V. We find that this procedure removes five points from the OGLE data, an additional 17 points from the μFUN Chile I data, seven points from the PLANET R data, two points from the PLANET I data, and none from the other data sets. The final renormalization factors are 1.96, 0.87, 2.2, and 1.4 for OGLE, μFUN Chile I, PLANET Tasmania I, and PLANET Chile R data, respectively. The other two data sets, μFUN Chile V and μFUN Israel I, do not require renormalization. This cleaned and renormalization data set is used in all fits reported in this paper and is shown in Figure 1. It contains 200 points from OGLE I, 167 from μFUN Chile I, 14 from μFUN Israel I, 11 from μFUN Chile V, 50 from PLANET Tasmania I, and 61 from PLANET Chile R.

Figure 2 shows the resulting likelihood contours in the π_E plane. The best fit is at $(\pi_{E,E}, \pi_{E,N}) = (0.0664, -0.0205)$. The contours are extremely elongated with their major axes almost perfectly aligned with the north-south axis. Gould et al. (1994) showed that short events would yield essentially one-dimensional parallax information because the Earth's acceleration vector is basically constant over the duration of the event. Hence, only a single parallax parameter can be measured
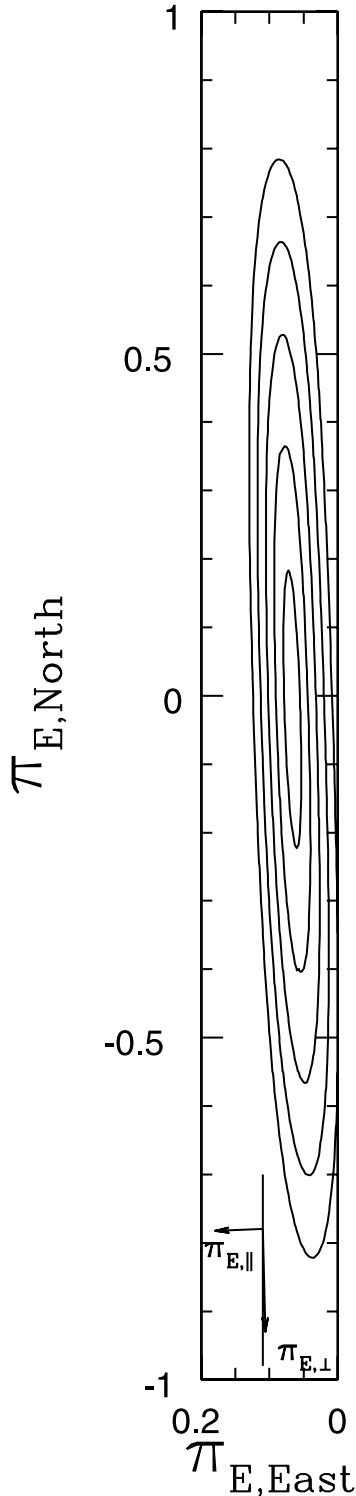
FIG. 2.—Likelihood contours ($\sigma = 1, 2, 3, 4, 5$) as a function of the vector parallax $\pi_{\rm E}$. The direction of the Sun's apparent acceleration is given by $\pi_{\rm E, \|}$. As expected from theory, the parallax is well constrained in this direction but poorly constrained in the orthogonal ($\pi_{\rm E, \perp}$) direction, which lies at an angle of $1°.769$ from the north-south axis (*vertical line segment*).

robustly, namely the magnitude of the asymmetry of the light curve. This yields information about the component of the projected lens-source relative velocity parallel to the Earth's acceleration (projected onto the plane of the sky) but not the perpendicular component. At the peak of the event, the position of the Sun (projected onto the plane of the sky; see eq. [6]

of Gould 2004) is $(s_E, s_N) = (-0.930\,{\rm AU}, 0.028\,{\rm AU})$, which means that the Earth is accelerating in the same direction. Hence, one expects the direction of maximum sensitivity (minor axis of the error ellipse) to be at a position angle $\tan^{-1}(-0.930/0.028) = 91°.725$ (north through east), which agrees quite well with the orientation ($91°.769$) shown in Figure 2. The event MOA-2003-BLG-37, which was also short ($t_{\rm E} \sim 42$ days) shows similar highly elongated parallax-error contours (Park et al. 2004).

Figures 1 and 2 both illustrate that the parallax effect in OGLE-2003-BLG-238 is weak. The residuals in Figure 1, which shows the fit without parallax, demonstrate that the asymmetry is quite subtle. Figure 2 shows that the error contours extend almost to the origin. That is, from Table 1, the addition of two parallax parameters reduces χ^2 from 510.6 to 478.3, a 5.5 σ effect.

4.3. Check for Parallax Degeneracies

Gould (2004) showed that microlensing events, particularly those with short timescales [$t_{\rm E} \lesssim (1/2\pi)$ yr], could be subject to a discrete four-fold degeneracy. One pair of degenerate solutions, which was previously discovered by Smith et al. (2003a), takes $u_0 \rightarrow -u_0$. The remaining parameters are then similar to the original parameters, with the differences being proportional to u_0. Since in the present case u_0 is extremely small, $u_0 = 2 \times 10^{-3}$, one expects that these two solutions would be virtually identical, and this proves to be the case.

The other pair of solutions arises from the "jerk-parallax" degeneracy, which predicts that if $\boldsymbol{\pi}_{\rm E} = (\pi_{\rm E, \|}, \pi_{\rm E, \perp})$ is a solution, then $\boldsymbol{\pi}'_{\rm E} = (\pi'_{\rm E, \|}, \pi'_{\rm E, \perp})$ is also a solution, with

$$\pi'_{\rm E, \|} = \pi_{\rm E, \|}, \qquad \pi'_{\rm E, \perp} = -(\pi_{\rm E, \perp} + \pi_{j, \perp}), \qquad (15)$$

where $\boldsymbol{\pi}_j$ is the "jerk parallax." In the approximation that the Earth's orbit is circular,

$$\pi_{j, \perp} = -\frac{4}{3} \frac{\rm yr}{2\pi t_{\rm E}} \frac{\sin \beta_{\rm ec}}{\left(\cos^2 \psi \sin^2 \beta_{\rm ec} + \sin^2 \psi\right)^{3/2}}, \qquad (16)$$

where $\beta_{\rm ec}$ is the ecliptic latitude of the source and $\psi = 69°$ is the phase of the Earth's orbit relative to opposition at the peak of the event. In the present case, the event is quite close to the ecliptic, $\beta_{\rm ec} \sim 0°.8$, so $\pi_{j, \perp} \sim -0.037$. Since $\pi_{\rm E, \perp} = 0.018$, this implies that $\pi'_{\rm E, \perp} = -(\pi_{\rm E, \perp} + \pi_{j, \perp}) = 0.017$, which is almost identical to $\pi_{\rm E, \perp}$. Hence, no degeneracy is predicted, and this expectation is confirmed by Figure 2, which shows a single minimum.

Note that for events seen right on the ecliptic, $\beta_{\rm ec} = 0$, equation (15) predicts $\pi'_{\rm E, \perp} = -\pi_{\rm E, \perp}$. Indeed, for this special case, the degeneracy is exact to all orders and not only to fourth order in the perturbative expansion as was derived by Gould (2004). That is, since the accelerated motion is exactly along the ecliptic, there is no way to distinguish whether the component of lens-source relative motion perpendicular to the ecliptic is toward the north or south. Since OGLE-2003-BLG-238 is very near the ecliptic, one would naively expect it to be strongly affected by this degeneracy. In fact, it is only because $\pi_{\rm E, \perp}$ is also very close to zero that the degeneracy is avoided.

The extreme axis ratio of the parallax-error ellipse, $\sigma(\pi_{\rm E, \perp})/\sigma(\pi_{\rm E, \|}) = 17$, confirms that the information about parallax is essentially one-dimensional, as predicted by Gould et al. (1994). However, it is not perfectly one-dimensional; while $\pi_{\rm E, \perp}$ is highly consistent with zero there is some constraint,

however weak, on this quantity. We search for the origin of this constraint within the context of the Gould (2004) formalism. For the limiting case (relevant here) of $u_0 \to 0$, $\pi_{E, \perp}$ first enters in the fourth-order term C_4 in the Taylor expansion $u^2 = \sum_i C_i(t - t_0)^i$. For sufficiently large $\pi_{E, \perp}$, $C_4 \sim (\alpha \pi_{E, \perp}/2)^2$, where $\alpha \sim (60 \text{ days})^{-2}$ is the apparent acceleration of the Sun at the peak of the event, divided by an AU (see eq. [20] of Gould 2004). Hence, for $u \gg u_0$ (i.e., essentially everywhere in the present case), $C_4(t - t_0)^4 \sim 0.04 u^4 \pi_{E, \perp}^2$, implying a perturbation $\Delta u \sim 0.02 u^3 \pi_{E, \perp}^2$. If we now consider $\pi_{E, \perp} = 0.4$ (roughly the 2 σ upper limit), and focus on $u \sim 1.5$ (where there is still a high density of 1% photometry and where $d \ln A/du \sim 0.3$ is still fairly high), then the amplitude of the effect is small, $\Delta A/A \sim (d \ln A/du) 0.02 u^3 \pi_{E, \perp}^2 \sim 3 \times 10^{-3}$, but still plausibly large enough given the large number of relatively high precision measurements.

5. NEGATIVE BLENDING

As seen from Table 1, the best nonparallax fit of the background flux for OGLE I band, μFUN Chile I band and V band, and PLANET I band are all negative. There are three potential reasons for such negative background fluxes: systematic photometry errors, unmodeled effects in the light curve that are absorbed by the blended flux parameter, and "negative flux" from unlensed sources. The first possibility is virtually ruled out by the fact that the negative background flux appears in so many unassociated light curves. The last possibility is not as ridiculous as it might first appear, because the dense Galactic bulge fields have a mottled background of turnoff and main-sequence stars. If the source happens to lie in a hole in this background, it will appear as negative F_b (Park et al. 2004). The $F_b/F_s = -5\%$ from the OGLE photometry (which has the most extensive baseline), would require a "hole" corresponding to a star 20 times fainter than the source, i.e., $I_{0, \text{hole}} \sim 17.6$ (see Fig. 3). This is a plausible brightness for a hole in the unresolved turnoff stars. Combining this value with the $F_b/F_s = -17\%$ measurement from PLANET R yields a color difference between the "hole" and the source,

$$\Delta(R - I) \equiv (R - I)_{\text{hole}} - (R - I)_s = -1.25 \pm 0.20, \quad (17)$$

whereas the expected value (given the source position in Fig. 3) is about $\Delta(R - I) \sim -0.5$. Hence this explanation is not completely self-consistent.

Because the effect of the blending parameter is even about the peak, it can absorb effects of other even parameters including F_s, ρ, u_0, and t_E. Since all of these are taken into account in the nonparallax fit (and its errors), these cannot be the cause. However, as pointed out by Smith et al. (2003a), microlens parallax can also mimic blending. Within the formalism of Gould (2004), the blending fraction is correlated with $\pi_{E, \perp}$, which is also an even parameter (see Park et al. 2004).

The best-fit parallax solution still contains negative background fluxes, although these are slightly reduced in magnitude relative to the nonparallax fit, while the errors are somewhat increased. The reduction reflects the absorption of some of the negative blending into $\pi_{E, \perp}$, while the larger errors reflect the covariance between F_b and $\pi_{E, \perp}$. However, since the negative blending is still detected with substantial significance, parallax cannot be the whole story. A "hole" in the mottled bulge background of turnoff stars remains the most plausible explanation for the negative blending, although as discussed above, this explanation is not perfect.
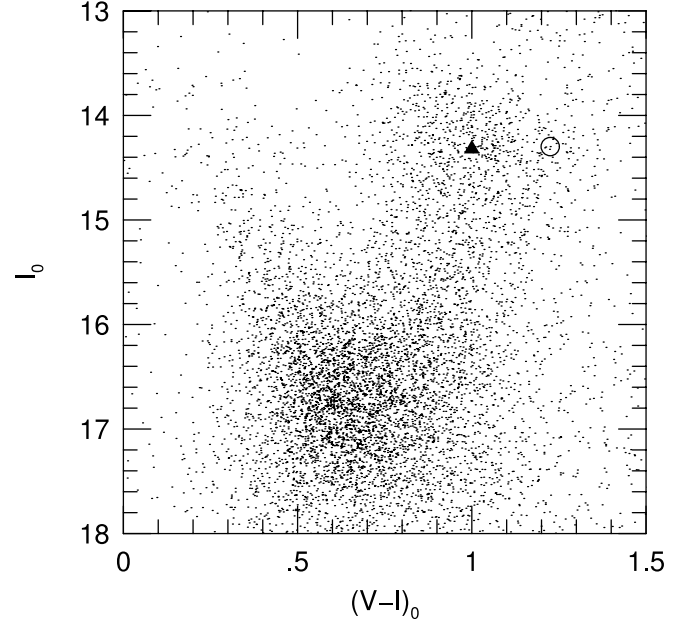

Fig. 3.—Uncalibrated color-magnitude diagram from μFUN data of a 6′ square around OGLE-2003-BLG-238 that has been translated to put the centroid of the clump (*triangle*) at its known position $[(V - I)_0, I_0]_{\text{clump}} = (1.00, 14.32)$. The unmagnified source (*circle*) is about 0.02 mag brighter and 0.22 mag redder than the clump.

6. ERROR DETERMINATION

We use Newton's method to find the minimum χ^2 with respect to the 18 parameters of the nonparallax model. This procedure utilizes the Fisher matrix and therefore automatically generates a covariance matrix and so linearized error estimates for all the parameters. We find, however, that Newton's method fails when we add the two parallax parameters, probably because the effect is too subtle to withstand the numerical noise induced by numerical differentiation of the finite source effects. We therefore hold $\boldsymbol{\pi}_E$ fixed at a grid of values and, at each one, minimize χ^2 with respect to the remaining 18 parameters. The resulting contours are shown in Figure 2. To estimate the errors we use the method of "hybrid statistical errors" given in Appendix D of An et al. (2002). First, Newton's method automatically yields $\tilde{c}_{ij}$, the covariance matrix of the model parameters (collectively a_i) with the two parameters $\boldsymbol{\pi}_E$ held fixed at their best-fit values. Next, we evaluate the two-dimensional covariance matrix $\hat{c}_{mn}$, where m, n range over the parameters $(\pi_{E, N}, \pi_{E, E})$, by fitting the contours in Figure 2 to a parabola. Third, we evaluate $\partial a_i/\partial a_m$, the change in the best-fit model parameter a_i as one of the parallax parameters is varied over the grid. Finally, we evaluate the covariance matrix c_{ij} by

$$c_{ij} = \tilde{c}_{ij} + \sum_{m, n = \pi_{E, N}, \pi_{E, E}} \hat{c}_{mn} \frac{\partial a_i}{\partial a_m} \frac{\partial a_j}{\partial a_n}. \quad (18)$$

7. ESTIMATES OF MASS AND DISTANCE

7.1. *Measurement of θ_E*

We determine the angular size of the source θ_* from the instrumental color-magnitude diagram (CMD) using the method developed by Albrow et al. (2000) and references therein, which is concisely summarized by Yoo et al. (2004). We measure the offsets in color and magnitude between the unmagnified source

star and the center of the clump giants, $\Delta I = I_s - I_{\mathrm{clump}} = -0.02$, $\Delta(V-I) = (V-I)_s - (V-I)_{\mathrm{clump}} = 0.22$. For the dereddened color and magnitude of the clump center, we adopt $[(V-I)_0, I_0]_{\mathrm{clump}} = (1.00, 14.32)$ (Yoo et al. 2004) then transform from $(V-I)_0$ to $(V-K)_0$ using the color-color relation of Bessell & Brett (1988). We obtain $[(V-I)_0, I_0]_s = (1.22, 14.30)$. Finally, using the color–surface-brightness relation of van Belle (1999), we obtain $\theta_* = 8.35 \pm 0.72\ \mu$as, where the error is dominated by the 8.7% scatter in the van Belle (1999) relation.

From the best-fit value $\rho = 0.0128$, we then obtain

$$\theta_{\mathrm{E}} = 652 \pm 56\ \mu\mathrm{as},$$

$$\mu_{\mathrm{rel}} = 6.20 \pm 0.54\ \mathrm{mas\ yr}^{-1} = 29.4 \pm 2.6\ \mathrm{km\ s}^{-1}\ \mathrm{kpc}^{-1}. \tag{19}$$

7.2. *Mass and Distance Estimates*

The best parallax fit for the event is $\pi_E = 0.0695$, which when combined with equations (3) and (19) yields

$$M = 1.15\ M_\odot \qquad \text{(best fit)}. \tag{20}$$

However, the errors are quite large. Figure 2 shows that at the $1\ \sigma$ level, π_{E} lies in the range $0.2256 > \pi_{\mathrm{E}} > 0.0552$, which implies

$$0.36 < M/M_\odot < 1.48 \qquad (1\ \sigma). \tag{21}$$

The same microlens parallax estimates lead (through eq. [3]) to a best relative parallax estimate of $\pi_{\mathrm{rel}} = 45\ \mu$as and a $1\ \sigma$ range of $147\ \mu\mathrm{as} > \pi_{\mathrm{rel}} > 35\ \mu$as. If one adopts a source distance of $D_s = 8$ kpc, this corresponds to a distance range $3.6\ \mathrm{kpc} < D_l < 6.3\ \mathrm{kpc}$.

At the $2\ \sigma$ level, $0.4180 > \pi_{\mathrm{E}} > 0.0434$, which leads to a mass range $0.19 < M/M_\odot < 1.86$ and a relative parallax range $273\ \mu\mathrm{as} > \pi_{\mathrm{rel}} > 28\ \mu$as, corresponding to $2.5\ \mathrm{kpc} < D_l < 6.5\ \mathrm{kpc}$. Therefore, the $2\ \sigma$ interval is consistent with most of the stellar range, but it does not provide any "new" information about the lens other than ruling out stellar-mass black holes and very late type M dwarfs and brown dwarfs. On the other hand, it does serve as a basic consistency check on the viability of the microlens mass measurements, since if the method were plagued by strong systematic errors one would not necessarily expect the estimated mass to lie in the stellar range.

7.3. *A Single Star?*

As noted in § 1, part of the motivation for microlensing mass measurements is that this is the only known way to directly measure the mass of single stars. But how confident can we be that OGLE-2003-BLG-238 is a single star? In a future paper, we will analyze the light curve for the presence of all types of companions to the lens, particularly planetary companions. However, by simple inspection of the light curve, it is possible to place rough limits on stellar-mass companions, i.e., those with mass ratios $q > 0.1$. No such companions are possible with separations (in units of θ_{E} of the *observed* lens) of $d \sim 1$, since there would be clearly visible caustic crossings.

As the separation is increased, the magnification pattern approaches a Chang-Refsdal lens with shear $\gamma = q_w/d_w^2$ (Chang & Refsdal 1979, 1984). The width of the Chang-Refsdal caustic in the limit of $\gamma \ll 1$ is $\ell \sim 4\gamma$. From inspection of the light curve and the fact that $u_0 \sim \rho/6$ (see Table 1), we can say that such a

caustic would certainly have been noticed if $\ell > \rho/2$. This implies a limit $d_w > (8q_w/\rho)^{1/2} = 25q_w^{1/2}$.

According to the so-called $d \to d^{-1}$ duality discovered by Dominik (1999) and further elaborated by Albrow et al. (2002), the central caustics of extremely close binaries mimic those of wide binaries. Keeping to the convention that the observed Einstein radius corresponds to the mass near the observed peak in the light curve (i.e., the combined mass of the binary in the close case but just the mass of one star in the wide case), one finds that $\gamma = d_c^2 q_c/(1 + q_c)^2$. Thus, by the same argument as above, $d_c < 0.04(1 + q_c)q_c^{-1/2}$. Combining these two arguments and making use of equation (19) implies that the entire range of companion projected separations $r_\perp$,

$$0.2\ \mathrm{AU}\ (q_c^{1/2} + q_c^{-1/2})\frac{D_l}{R_0} < r_\perp < 85\ \mathrm{AU}\ q_w^{1/2}\frac{D_l}{R_0}$$

$$\text{(excluded companions)}, \tag{22}$$

is excluded. Here D_l is the distance to the lens and $R_0 = 8$ kpc. Hence, if the lens has a stellar companion, it is either extremely close or very far away.

8. FUTURE PROSPECTS

To date, microlensing mass measurements of single stars have depended on very rare combinations of circumstances. The problem is somewhat more severe than was outlined in § 1. There we noted that π_{E} and θ_{E} were separately measured only infrequently, so combined measurements are even more infrequent. However, for single stars, the events most likely to show the parallax effects from which one could measure π_{E} are also the least likely to show the finite-source effects from which one could measure θ_{E}. That is, microlens parallax measurements generally require long events, $t_{\mathrm{E}} \gtrsim (1/2\pi)$ yr, which tend to favor large masses, since $t_{\mathrm{E}} \propto M^{1/2}$. But the probability of significant finite-source effects (i.e., $u_0 \lesssim \rho$) scales as $\rho = \theta_*/\theta_{\mathrm{E}}$, which favors small masses, since $\theta_{\mathrm{E}} \propto M^{1/2}$. The combination of large t_{E} and small θ_{E} implies low relative proper motion, $\mu_{\mathrm{rel}} = \theta_{\mathrm{E}}/t_{\mathrm{E}}$.

Actually, neither of the two single-star events with microlens mass measurements meets this criterion. OGLE-2003-BLG-238 has $\mu \sim 6$ mas yr^{-1}, which is a typical value for disk lenses seen against the bulge and is substantially higher than the proper motions expected for bulge-bulge events. MACHO-LMC-5 has $\mu \sim 20$ mas yr^{-1}, which of course is extremely fast. What can be learned about the future prospects for single-star mass measurements from the failure of both of these events to "fit the mold"?

OGLE-2003-BLG-238 was not long enough to obtain a good microlens parallax measurement. That is, only the $\pi_{\mathrm{E},\parallel}$ component of the microlens parallax vector $\boldsymbol{\pi}_{\mathrm{E}}$ can really be said to have been "measured." The other ($\pi_{\mathrm{E},\perp}$) component was only grossly constrained. Regarding MACHO-LMC-5, it was neither long enough for a very accurate measurement of $\boldsymbol{\pi}_{\mathrm{E}}$, nor did it exhibit the finite source effects that are normally required to measure θ_{E}. The fact is that auxiliary, nonmicrolensing data were needed to measure θ_{E} for this event. That is, the source and lens were separately resolved six years after the event, and from the measurement of their separation, Alcock et al. (2001) were able to deduce μ_{rel}, which when combined with microlensing data yielded θ_{E}.

This experience with MACHO-LMC-5 points to one future route to microlens mass measurements: give up altogether on measuring θ_{E} from the microlensing events; instead, just focus

on long events with good parallax measurements and measure θ_E from postevent astrometry. Han & Chang (2003) estimated that 22% of disk-bulge events could be resolved 10 years after the event, assuming a resolution of 50 mas.

Alcock et al. (2001) proposed a second route to measuring the mass of MACHO-LMC-5: use the fact that the source was already resolved to measure both the lens-source relative parallax, π_{rel}, and the lens-source relative proper motion, μ_{rel}. One sees directly from equation (1) that if these two measurements are combined with a measurement of t_E, one obtains the lens mass, M. Indeed, this would be a variant of the original idea of Refsdal (1964) to determine single-star masses by first finding nearby stars passing close to the line of sight of more-distant stars and by then obtaining π_{rel}, and the angular deflection $\Delta\theta_{rel}$ at the impact parameter $b = u_0\theta_E$, all from astrometry. The only difference being that for these nearby lenses, which generally pass well outside the Einstein ring ($u_0 \gg 1$), $\theta_E = (b\Delta\theta_{rel})^{1/2}$, is determined directly from astrometry rather than from the combination of astrometric (μ_{rel}) and photometric (t_E) parameters employed by Alcock et al. (2001).

Yet a third route is suggested by the experience of OGLE-2003-BLG-238. In spite of its short duration, the microlens parallax is well measured in one direction. If the lens could be resolved by postevent imaging, this would not only yield the *magnitude* of the proper motion μ_{rel} but also its *direction*. Since the directions of μ_{rel} and π_E are the same, the proper-motion measurement would at the same time resolve the parallax degeneracy. It may prove difficult to apply this method to OGLE-2003-BLG-238 itself because (from Table 1), the source is so much brighter than the lens. However, Ghosh et al. (2004) argue that another event, OGLE-2003-BLG-175/MOA-2003-BLG-45, shows excellent promise for yielding a mass with this method.

Finally, a fourth route has been proposed by several authors (Agol et al. 2002; Delplancke et al. 2001; Dalal & Lane 2003). For very massive lenses, primarily black holes, the events will generally be long enough to measure π_E, while θ_E may be large enough to measure it using precise astrometry from the deviation of the centroid of lensed light relative to the source position. F. Delplancke (2004, private communication) expects that she and her team at the Very Large Telescope will achieve the required high precision for $K < 11$, 13, and 16 sources in 2004, 2005, and 2006, respectively.

In the longer term, it should be possible to measure single-star masses using the *Space Interferometry Mission* (*SIM*) in two distinct ways. First, *SIM*'s high (4 μas) precision will allow one to carry out the original Refsdal (1964) proposal, provided appropriate lens-source pairs can be found (Paczyński 1998; Gould 2000; Salim & Gould 2000). Second, for microlensing events generated by distant lenses (whether luminous or not) and for sufficiently bright sources, it will be possible for *SIM* to routinely measure θ_E from the centroid displacement discussed above (Boden et al. 1998; Paczyński 1998). On the other hand, since *SIM* will be in solar orbit, comparison of *SIM* and ground-based photometry of the event will yield microlens parallaxes according to the method of Refsdal (1966) and Gould (1995). Approximately 200 such measurements should be feasible with the 1200 hours of *SIM* time that has been allocated to this project (Gould & Salim 1999).

REFERENCES

Agol, E., Kamionkowski, M., Koopmans, L. V. E., & Blandford, R. D. 2002, ApJ, 576, L131
Albrow, M. D., et al. 1998, ApJ, 509, 687
———. 2000, ApJ, 535, 176
———. 2002, ApJ, 572, 1031
Alcock, C., et al. 1993, Nature, 365, 621
———. 1997, ApJ, 491, 436
———. 2001, Nature, 414, 617
An, J. H., et al. 2002, ApJ, 572, 521
Aubourg, E., et al. 1993, Nature, 365, 623
Bessell, M. S., & Brett, J. M. 1988, PASP, 100, 1134
Boden, A. F., Shao, M., & Van Buren, D. 1998, ApJ, 502, 538
Chang, K., & Refsdal, S. 1979, Nature, 282, 561
———. 1984, A&A, 130, 157
Dalal, N., & Lane, B. F. 2003, ApJ, 589, 199
Delplancke, F., Gorski, K. M., & Richichi, A. 2001, A&A, 375, 701
DePoy, D. L., et al. 2003, SPIE, 4841, 827
Dominik, M. 1998, A&A, 329, 361
———. 1999, A&A, 349, 108
Drake, A. J., Cook, K. H., & Keller, S. C. 2004, ApJ, 607, L29
Ghosh, H., et al. 2004, ApJ, 615, 450
Gould, A. 1992, ApJ, 392, 442
———. 1994, ApJ, 421, L71

Gould, A. 1995, ApJ, 441, L21
———. 2000, ApJ, 532, 936
———. 2004, ApJ, 606, 319
Gould, A., Bennett, D. P., & Alves, D. R. 2004, ApJ, 614, 404
Gould, A., Miralda-Escudé, J., & Bahcall, J. N. 1994, ApJ, 423, L105
Gould, A., & Salim, S. 1999, ApJ, 524, 794
Han, C., & Chang, H.-Y. 2003, MNRAS, 338, 637
Paczyński, B. 1986, ApJ, 304, 1
———. 1998, ApJ, 494, L23
Park, B. G., et al. 2004, ApJ, 609, 166
Refsdal, S. 1964, MNRAS, 128, 295
———. 1966, MNRAS, 134, 315
Salim, S., & Gould, A. 2000, ApJ, 539, 241
Schechter, P. L., Mateo, M., & Saha, A. 1993, PASP, 105, 1342
Smith, M., Mao, S., & Paczyński, B. 2003a, MNRAS, 339, 925
Smith, M., Mao, S., & Woźniak, P. 2003b, ApJ, 585, L65
Udalski, A. 2003, Acta Astron., 53, 291
Udalski, A., et al. 1993, Acta Astron., 43, 289
van Belle, G. T. 1999, PASP, 111, 1515
Witt, H., & Mao, S. 1994, ApJ, 430, 505
Woźniak, P. R. 2000, Acta Astron., 50, 421
Yoo, J., et al. 2004, ApJ, 603, 139